

Paper published as:

Tancredi, U.; Grassi, M.; Corrado, F.; Filippone, E. & Verde, L. (2010), 'A hybrid approach to robustness analyses of flight control laws in re-entry applications', *Acta Astronautica* **66**(9-10), 1388--1398.

<http://dx.doi.org/10.1016/j.actaastro.2009.10.033>

A HYBRID APPROACH TO ROBUSTNESS ANALYSES OF FLIGHT CONTROL LAWS IN RE-ENTRY APPLICATIONS

Urbano Tancredi

Department for Technologies, University of Naples "Parthenope," Napoli, Italy
urbano.tancredi@uniparthenope.it

Michele Grassi

Department of Aerospace Engineering, University of Naples "Federico II," Napoli, Italy
michele.grassi@unina.it

Federico Corraro, Edoardo Filippone, and Leopoldo Verde

Italian Aerospace Research Center (CIRA), Flight Systems Department, Capua (CE), Italy
f.corraro@cira.it , e.filippone@cira.it , l.verde@cira.it

ABSTRACT

The present paper aims at improving the efficiency of the robustness analyses of flight control laws with respect to conventional techniques, especially when applied to vehicles following time-varying reference trajectories, such as in an atmospheric re-entry. A nonlinear robustness criterion is proposed, stemming from the Practical Stability framework, which allows dealing effectively with such cases. A novel approach is presented, which exploits the convexity of linear time-varying systems, coupled to an approximate description of the original nonlinear system by a certain number of its time-varying linearizations. The suitability of the approximating systems is evaluated in a probabilistic fashion making use of the Unscented Transformation technique. The method effectiveness and potentials are ascertained by application to the robustness analysis of the longitudinal flight control laws of the Italian Aerospace Research Center (CIRA) experimental vehicle USV.

1 INTRODUCTION

A general problem that arises during the design phase of an aerospace system and when verifying the control performance and stability robustness is to assess vehicle compliance with a set of mission requirements, in face of uncertain parameters ranging in given subsets. In particular, during the Flight Control Laws (FCL) design and verification phases, robustness analyses are frequently required in order to drive the FCL refinement process. In these cases, it is useful to estimate the uncertainty ranges that guarantee compliance to a requirement. This allows, for instance, establishing the limiting operating conditions for an FCL candidate, or meaningfully selecting a limited set of worst cases for the control design upgrade, thanks also to a simpler understanding of the underlying physics and the effects that these uncertainty combinations produce on the trajectory. The present paper deals with the problem of analyzing the robustness with respect to parametric uncertainties of FCL for vehicles performing an atmospheric re-entry. This is a challenging application for robustness analyses, because, among others, of stringent requirements on the trajectories that can be safely flown, and of significant uncertainties on the design parameters, most notably on aerodynamic coefficients.

State-of-the-art robustness analysis techniques mainly exploit the possibility of describing the nonlinear system dynamics applying the small perturbation theory around pre-defined stationary equilibrium points. However, given the unsteady nature of the re-entry trajectory, the extended range of flight regimes, the large uncertainty and disturbances ranges, the vehicle trajectory can be poorly represented assuming trimmed stationary flight or quasi-steady maneuvers, which calls for different approaches. In addition, in these applications, uncertain perturbations that do not vanish on the system reference trajectory are typically present. This implies that the classical concept of stability of equilibrium points cannot be applied, and the system robustness is better analyzed in an input-output setting [1].

Presently, when analyzing a re-entry mission, Monte Carlo based simulations are customary used with the drawback to not get useful information for vehicle or control system design refinement and or modification, but giving only a global assessment of the system compliance to a requirement, assuming pre-defined statistic characterization of the uncertain parameters (which are not always available).

For these reasons, Monte Carlo techniques are not suited to perform robustness analyses in the early phases of the FCL design cycle, where it is essential to provide information to support the design refinement process. The customary employed approach in this framework is an extension of LTI systems – based robustness analysis techniques also to these time-varying applications, making use of frozen-time linearization theory. However, frozen-time linearization has severe inherent limitations [2], and, as non-vanishing uncertainties are taken into account, this approach lacks coherence. This implies that even an effective LTI-based robust stability analysis approach can deliver only indicative results, often heavily conservative, when used in the context of the considered applications. Therefore, previously unidentified criticalities or excessively conservative design choices can emerge in the final stages of the FCL design and verification loop, calling for additional time-consuming iterations. This results into an inefficient design process, in which extensive nonlinear simulations and physical phenomenon understanding are continuously required to support the robustness analyses results, as in the Space Shuttle case [3].

A novel approach to robustness analysis in the uncertain parameters space is presented, aimed at improving the efficiency of the design upgrade process with respect to conventional techniques, especially when applied to re-entry applications. This is done by delivering feedback on the causes of requirement violation for supporting the FCL design refinement, and thus the approach is intended to be used before robustness is finally assessed with MC analysis. To this end, the robustness analysis problem is formulated as determining the subset of the uncertain parameters domain in which a criterion translating mission requirements is matched. This allows estimating the uncertainty ranges that guarantee compliance to such requirements. The practical stability concept [4] is proposed as a robustness criterion, which allows handling rigorously re-entry applications peculiarities. However, no well-established approaches exist for the practical stability analysis of a nonlinear system. Current methods for analyzing the practical stability property suffer of significant drawbacks when considered from an applicability perspective. Indeed, examples of their application in cases of practical interest within the robustness analysis context are quite scarce.

In a previous work by the authors [5], this robustness analysis problem was approached by combining practical stability analysis methods for Linear Time Varying (LTV) systems with an approximate description of the original nonlinear system by a certain number of its time-varying linearizations. However, determination of which time-varying linearizations were appropriate for approximating the nonlinear system was found to be an intractable problem, and the approximation was thus performed heuristically. The present paper advances the previous work by employing probabilistic techniques to avoid introducing heuristic assumptions. In particular, suitability of the LTV approximating systems is evaluated in a probabilistic fashion making use of the Unscented Transformation technique [6]. Then, the practical stability analysis is performed by means of a deterministic approach exploiting the convexity-preserving nature of LTV systems. As a result, we obtain a hybrid probabilistic – deterministic approach, capable of solving the robustness analysis problem with no heuristic assumptions. The method effectiveness and potentials are ascertained by application to a problem of practical engineering interest, within the framework of the Italian Aerospace Research Center (CIRA) experimental vehicle USV [7].

2 PROBLEM SETTING

In the following, we briefly recall the robustness analysis problem setting and the practical stability criterion. For a more detailed description, the interested reader is referred to [5].

In order to provide a flight dynamics description suitable to winged vehicles performing an atmospheric re-entry, let us consider the following dynamical system:

$$x = f(t, x, \pi) \quad y = g(t, x, \pi) \quad (1)$$

where $x \in \mathfrak{R}^n$ is the state vector, $y \in \mathfrak{R}^m$ is the output vector, $f(\cdot)$ is the nonlinear dynamics function, $g(\cdot)$ is the output function, and π is the vector of parametric uncertainties. Let us assume to have a finite number p of parametric uncertainties, with zero nominal value, and that the uncertainties are enclosed in a bounded set $\Pi \subseteq \mathfrak{R}^p$. Dependency on an input signal $u(\cdot)$ is taken into account within the $f(\cdot)$ and $g(\cdot)$ functions. The above model is well suited to represent the typical closed-loop augmented dynamics of an atmospheric re-entry vehicle. For instance, the input signal $u(\cdot)$ can describe the FCL conventionally used for atmospheric re-entry applications, i.e. a gain-scheduled inner-loop PID control scheme coupled with a time-varying guidance law, possibly dependent on the system state as well. In this case, indeed, the gain scheduling can be taken into account by the dependency on the state variables (and time if needed), and the PID action by dependencies on the state, on its time integral (which adds up to the open-loop system's state) and derivative, respectively.

Given the applications we wish to describe, we refer to time-varying reference trajectories rather than stationary operating conditions. This could be due to the lack of stationary equilibrium solutions for system (1), as in the case of an un-powered re-entry vehicle in steep gliding flight. In addition, these trajectories are usually defined on a finite-time domain, which we will explicitly take into account by assuming that $t \in [0, T]$, where the initial epoch is taken equal to zero for simplicity and T

is a finite positive real number. The reference trajectory, which is denoted with the \sim superscript, is thus time varying on a compact time domain, and satisfies the following equations.

$$\tilde{x}(t) := \tilde{x}_0 + \int_0^t f(\tau, \tilde{x}, 0) \cdot d\tau \quad \forall t \in [0, T] \quad (2a)$$

$$\tilde{y}(t) := \tilde{y}_0 + \int_0^t g(\tau, \tilde{x}, 0) \cdot d\tau \quad \forall t \in [0, T] \quad (2b)$$

The common approach to determine system (1) robustness is to analyze the uncertainties effect in modifying the system dynamics around the reference trajectory. It is thus convenient to rearrange the system dynamics in terms of variations with respect to such trajectory. The resulting variations dynamics, obtained as the difference between the nominal and actual dynamics, are nonlinear, time-varying on a bounded time domain, and admit a stationary equilibrium point at the origin in nominal conditions. This manipulation of the system's equations introduces a fictitious time-variance induced by the reference trajectory, which becomes an equilibrium point for the new representation. In this way, one can define robustness criteria based on the classical Lyapunov stability property of equilibrium points. However, this approach cannot be always extended to analyze the system robustness to uncertainties. More precisely, the persistency of the variations system fictitious equilibrium point with respect to nonzero uncertainties is a critical point. When nonzero uncertainties induce perturbations on the dynamics that modify the equilibrium point, denoted as non-vanishing in the open literature [1], robustness criteria based on the stability of equilibrium points cannot be applied. In these cases, the system robustness shall be analyzed in an input-output setting. We emphasize that this case typically occurs when analyzing the longitudinal dynamics of re-entry vehicles. For instance, a nonzero uncertainty on the drag coefficient causes a change of the system trajectory, thus inducing a non-vanishing perturbation on the variations system dynamics.

The nonlinear robustness criterion proposed in the present work is based on the Practical Stability and/or Finite-Time Stability concepts, whose detailed description can be found in [4],[8]. This type of stability requires only the inclusion of the system trajectories in a pre-specified subset of the state space, possibly time-varying, in face of bounded initial state displacements and disturbances. As opposed to the classical Lyapunov stability concept, which is qualitative in nature, it does not require the existence of any equilibrium point, and is independent from Lyapunov stability, in the sense that one neither implies nor excludes the other. The practical stability criterion is inherently well suited to the applications of interest. Indeed, it allows dealing with non-vanishing uncertainties, to take explicitly into account system (1) time domain finiteness, and to use robustness criteria directly linked to the original mission or system requirements, which are typically expressed in terms of trajectory tracking performances. Indeed, the latter can be easily enforced by requiring the inclusion of the system trajectories in a pre-specified time-varying subset of the state space determined by the tracking requirements, to which we refer as the admissible solutions tube, $S_R(t)$.

In order to simplify the criterion formulation, and because the main focus of the present paper is on addressing the uncertainties effects, let us assume the initial state to be perfectly known and equal to the reference one. In other words, the perturbed output trajectory $y(t, \pi)$ is defined as a trajectory of system (1) output that starts at $t = 0$ in $y(0) = y|_{\square_0}$, under the constant input π . The robustness criterion is thus described as a Boolean property P , being true when the criterion is met.

$$P(\pi) = \begin{cases} 1 & y(t; \pi) \in S_R(t) \quad \forall t \in [0, T] \\ 0 & \exists t \in [0, T] : y(t; \pi) \notin S_R(t) \end{cases} \quad (3)$$

In a FCL design context, a valuable information is to distinguish the combinations of uncertain parameters within Π for which the property holds, from those for which the property is not verified (i.e. is false). For instance, it allows for global coverage in the uncertainties domain of the FCL performance, as opposed to classical worst-case analysis that identifies only a limited number of points in Π . This in turn aids the FCL upgrade by simplifying the physical understanding of the causes for poor performance. With this in mind, the FCL clearance task is stated as determining the set Π_{Adm} , subset of Π , which is made of all the ‘‘admissible’’ uncertainties, that is, all uncertainties satisfying the robustness criterion.

$$\Pi_{Adm} := \{ \pi \in \Pi \mid P(\pi) = 1 \} \quad (4)$$

In this setting, the robustness analysis task may be viewed as solving the following problem.

Problem 1. Given system (1), a bounded set $\Pi \subseteq \mathfrak{R}^p$ such that $\pi \in \Pi$, a time-varying compact set $S_R(t)$ (admissible solutions tube), and the property P (3), determine the set Π_{Adm} (4).

3 SOLUTION APPROACH

In order to simplify Problem 1 solution, we introduce the following restricting assumptions.

Assumption 1. The functions in Eq.(1), $f(\cdot)$, and $g(\cdot)$, are differentiable in t , x and π over relevant domains.

Assumption 2. The unknown parameters range in a p -dimensional hyper-rectangle Π .

$$\Pi := [\underline{\pi}_1, \bar{\pi}_1] \times \dots \times [\underline{\pi}_p, \bar{\pi}_p] \quad (5)$$

Assumption 3. The required solutions tube is an m - dimensional hyper-rectangle for all $t \in [0, T]$

$$S_R(t) := [\underline{S}_{1R}(t), \bar{S}_{1R}(t)] \times \dots \times [\underline{S}_{mR}(t), \bar{S}_{mR}(t)] \quad (6)$$

Various approaches exist being capable to deal with the Practical Stability analysis of a nonlinear dynamical system. The most prominent are based either on the definition of Lyapunov-like functions (see [8] and the references therein), or on the positively invariance of a set [9]. Even though a wide literature exists concerning theoretical results on practical stability, all these approaches suffer of significant drawbacks when considered from an applicability perspective, including cases where the system's dynamics is linear, although time-varying. Indeed, the abundance of theoretical results on Practical Stability analysis methods it is not balanced by examples of their application in cases of practical interest, at least within the robustness analysis context, which are quite scarce.

In the following, an original approach has been developed, inspired by the ‘‘hybridization’’ approach, which has been recently proposed for the performance verification of nonlinear systems [10]. The essence of the hybridization approach is to study a complex system by approximating it with simpler systems, for which well-assessed analysis tools exist, and to take into account the approximation error in the problem solution. This is done in the present context by substituting the nonlinear vehicle dynamics with numerically-generated time-varying linearizations in off-nominal conditions. Then, the LTV systems' practical stability is assessed over a whole uncertainty region, by performing numerical simulations only at suitably selected uncertainty combinations and exploiting the convexity preservation of its trajectories.

More precisely, let us consider a partition of the uncertainties domain, $\{\Pi_k\}$, such that each block Π_k is hyper-rectangular as well. We then define a collection of LTV systems, each one approximating the nonlinear system in a single block Π_k . In particular, each LTV system is obtained linearizing the nonlinear system around its trajectory under the geometrical center of Π_k , which we denote as π_k^0 . The corresponding nonlinear state and output trajectories are denoted as x_k^0 and y_k^0 as well. The equations that describe the dynamics of the LTV system defined on the generic Π_k (x_{Lk} and y_{Lk} denote the LTV's state and output variables, respectively) are thus:

$$\dot{x}_{Lk} = \dot{x}_k^0 + A_k(t) \cdot (x_{Lk} - x_k^0) + G_k(t) \cdot (\pi - \pi_k^0) \quad (7a)$$

$$y_{Lk} = y_k^0 + C_k(t) \cdot (x_{Lk} - x_k^0) + D_k(t) \cdot (\pi - \pi_k^0) \quad (7b)$$

where the A_k , G_k , C_k , and D_k matrixes are obtained applying first order expansion of the nonlinear functions in Eq. (1) around x_k^0 , π_k^0 . We can then define a function on the whole uncertain parameters domain Π that collects all the output trajectories of the approximating LTV systems, i.e. an $y_L: [0, T] \times \Pi \rightarrow \mathcal{R}^m$, such that $y_L(t; \pi) := y_{Lk}(t; \pi)$, for $\pi \in \Pi_k$. The error made in approximating the nonlinear system by the LTV ones is quantified by means of the weighted L_∞ norm distance between the two trajectory functions:

$$d(\pi) := \|y(t, \pi) - y_L(t, \pi)\|_\infty^b \quad (8)$$

The main idea that allows shifting the robustness analysis problem to the LTV systems is to find a partition $\{\Pi_k\}_{Lin}$ such that the approximation error is below a pre-specified error tolerance ε in all Π :

$$\{\Pi_k\}_{Lin} : \max_{\Pi} d(\pi) \leq \varepsilon \quad (9)$$

At this point, reducing the admissible solutions tube of the maximum error made in approximating the nonlinear system, the robustness analysis problem may be solved on the approximating LTV systems. More precisely, denote as B_ε the closed ball in \mathcal{R}^m with respect to the above norm, with radius equal to ε , denote with the \oplus symbol the Minkowski sum of two sets, and define a reduced admissible solutions tube, obtained by shrinking appropriately $S_R(\cdot)$.

$$S'_R(t) : S'_R(t) \oplus B_\varepsilon = S_R(t) \quad \forall t \in [0, T] \quad (10)$$

The $S'_R(\cdot)$ complying to Eq.(10) can be easily determined since $S_R(t)$ is hyper-rectangular at each time epoch. In this case, being B_ε hyper-rectangular as well by definition, $S'_R(\cdot)$ can be obtained simply by component-wise difference of $S_R(\cdot)$ and B_ε . It is straightforward to verify that, if y_L is computed on $\{\Pi_k\}_{Lin}$, the following holds:

$$y_L(t; \pi) \in S'_R(t) \quad \forall t \in [0, T] \Rightarrow P(\pi) = 1$$

Thus, if Problem 1 is solved on such a collection of LTV systems using $S'_R(\cdot)$ instead of $S_R(\cdot)$, one can obtain a conservative approximation of Π_{Adm} , in the sense that the computed admissible region will be included in the actual Π_{Adm} . From the previous discussion, it is clear that the amount of conservativeness in estimating Π_{Adm} is linked to the error tolerance ε , decreasing as it decreases.

Summarizing, the above approach requires to:

- Find a partition $\{\Pi_k\}_{Lin}$ in whom the nonlinear trajectories are well-approximated, as previously discussed, by those of its linearizations (7)
- Solve Problem 1 on the LTV systems, reducing the admissible solutions tube by Eq.(10)

The next sections discuss these two points separately.

3.1 Determination of $\{\Pi_k\}_{Lin}$

The partition in which the approximation error function $d(\cdot)$ is below the linearization threshold ε is determined exploiting the differentiability of the nonlinear system's function. In particular, since

$$\lim_{\pi \rightarrow \pi_k^0} \|y(t; \pi) - y_{Lk}(t; \pi)\|_{\infty} = 0$$

Then, for any π_k^0 and any $\varepsilon > 0$, it will exist a sufficiently small Π_k centered on π_k^0 , such that the approximation error function $d(\cdot)$ is smaller than ε on Π_k .

Following this observation, we propose to determine the desired partition $\{\Pi_k\}_{Lin}$ by repeatedly shrinking the Π_k sets until the approximation error is below the tolerance. This is obtained by recursively applying an isotropic bisection technique. More precisely, the isotropic bisection procedure splits a single p -dimensional hyper-rectangle in 2^p hyper-rectangular subsets, collectively exhaustive and mutually exclusive with respect to the “father” set. These “sons” are generated bisecting in each of the p dimensions the father hyper-rectangle's edges. This procedure is recursively applied on a block-wise base, in order to provide a somehow adaptive $\{\Pi_k\}_{Lin}$ partition at the end of the whole process. More precisely, only the subsets Π_k for which the approximation error is found to be higher than ε are further bisected, thus avoiding to refine the regions in the uncertain parameters space in which the nonlinear system is already “well” linearized. The technique that allows determining the value of the approximation error on a hyper-rectangular subset Π_k is described in the following section.

3.1.1 Evaluation of Nonlinear Trajectories Approximation Error

The major challenge in determining a partition suitable for approximating the nonlinear system trajectories with those of its time-varying linearizations resides in the evaluation of the $d(\cdot)$ function upper bound over Π_k , i.e. in determining if for all π in a given hyper-rectangle Π_k the distance between nonlinear and linear trajectories is within the error tolerance. Few results exist in the open literature that allow relating the time responses of a nonlinear system to those of its linearization by quantitative means (e.g. [11], [12]). These approaches conservatively bound from above a certain measure of the trajectories distance by maximizing some nonlinear time-varying function over a vector space. They thus either solve an optimization problem, with related computational complexity, or require prior knowledge of the maximum bound, such as the Lipschitz constant [10] or the maximum bound of second order derivatives [10],[11]. The latter methods, however, provide bounds on the trajectory distance that are typically exponentially increasing with time. This implies that in practice they can be used for time horizons of limited duration w.r.t. the system time-scales, which is not the case of re-entry applications. Alternative approaches have been proposed, which estimate the approximation error introducing some heuristics. In [13], the linear system is considered a valid approximation within a norm-ball, whose radius is fixed by heuristics depending on the linear trajectory characteristics. In [5], the approximation error over a polytope in the parameters space is estimated by its maximum value over the polytope's vertices, assuming that the polytope is sufficiently smaller than the scale at which the system exhibits significant nonlinear behavior so that the maximum error always occurs in a vertex.

In the present paper, we propose to evaluate the approximation error by probabilistic methods. In particular, fictitiously introducing a statistical description of the uncertain parameters in the generic Π_k , we accept the risk of the approximation error being higher than the tolerance in a subset of Π_k having small probability measure. Let us denote, for the sake of brevity, as $d_k(\cdot)$ the restriction of the $d(\cdot)$ on Π_k . We consider the nonlinear system as well approximated in Π_k if the risk of $d_k(\cdot)$ being higher than the error tolerance is smaller than a threshold, which we fix to 6%, that is:

$$\Pi_k : \Pr\{d_k(\pi) > \varepsilon\} \leq 0.06 \quad \Rightarrow \quad \Pi_k \in \{\Pi_k\}_{Lin} \quad (11)$$

Without introducing any assumption on the probability distribution of $d_k(\cdot)$, we can then use the one-sided Chebyshev inequality (given $d_k(\cdot)$ positiveness) to translate Eq.(11) in:

$$\Pi_k : E[d_k] + 4\sqrt{\text{Var}[d_k]} \leq \varepsilon \Rightarrow \Pi_k \in \{\Pi_k\}_{Lim}$$

where $E[d_k]$ and $\text{Var}[d_k]$ are the mean and variance of $d_k(\cdot)$. In order to determine these values, we use the Scaled Unscented Transformation (SUT), first introduced in [14], to which we refer the interested reader. The unscented transformation consists in estimating the mean and covariance of a nonlinear function f , by computing the mean and covariance of the discrete set of points obtained propagating a set of deterministically chosen points through the nonlinear function f .

Let us consider a generic hyper-rectangle Π_k , $\Pi_k := [\underline{\pi}_{1k}, \bar{\pi}_{1k}] \times \dots \times [\underline{\pi}_{pk}, \bar{\pi}_{pk}]$. We fictitiously assume π to be uniformly distributed over Π_k . The probability density function $U_k(\pi)$ is thus:

$$U_k(\pi) := \begin{cases} 1 / \prod_{i=1}^p l_{ki} & \text{if } \pi \in \Pi_k \\ 0 & \text{otherwise} \end{cases}$$

where l_{ki} stands for the linear length of Π_k in each principal direction, i.e. $l_{ki} := \bar{\pi}_{ki} - \underline{\pi}_{ki}$. The resulting mean and covariance matrix are:

$$E_k = \pi_k^0 ; \text{Cov}_k = \frac{1}{12} \cdot \text{diag} \{l_{k1}^2, \dots, l_{kp}^2\}$$

Using the SUT, we may estimate $d_k(\cdot)$ mean and variance (since it is a scalar function). According to [14], we choose a series of $2p+1$ points Θ_{ki} in Π_k , symmetrically distributed around the mean π_k^0 , obeying the following relationships:

$$\begin{aligned} \Theta_{ki} &= \pi_k^0 & i &= 0 \\ \Theta_{ki} &= \pi_k^0 + \left(\sqrt{(p+\lambda)\text{Cov}_k} \right)_i & i &= 1, \dots, p \\ \Theta_{ki} &= \pi_k^0 - \left(\sqrt{(p+\lambda)\text{Cov}_k} \right)_{i-p} & i &= p+1, \dots, 2p \end{aligned}$$

Where $\lambda = \alpha^2(p+\kappa) - p$, α and κ are tunable parameters, and $\left(\sqrt{(p+\lambda)\text{Cov}_k} \right)_i$ stands for either the row or the column of such matrix, depending on the square root used to compute it. Each point has an associated weight for computing the mean and variance of the $d_k(\cdot)$ function, and the first point Θ_{k0} has two weights, one for computing the mean and one for the variance. Denoting with $W_i^{(m)}$ the weights for computation of $E[d_k]$, and with $W_i^{(c)}$ the weights for computation of $\text{Var}[d_k]$, the following hold.

$$W_0^{(m)} = \lambda / (p+\lambda) ; W_0^{(c)} = W_0^{(m)} + (1 - \alpha^2 + \beta)$$

$$W_i^{(m)} = W_i^{(c)} = 1 / [2(p+\lambda)] \quad i = 1, \dots, 2p$$

The mean and variance of the $d_k(\cdot)$ function can then be estimated as the weighted average and outer product of the transformed points:

$$E[d_k] = \sum_{i=0}^{2p} W_i^{(m)} d_k(\Theta_{ki})$$

$$\text{Var}[d_k] = \sum_{i=0}^{2p} W_i^{(c)} \{E[d_k] - d_k(\Theta_{ki})\}^2$$

The SUT has three tunable parameters, α , β , and κ . The latter has been fixed equal to zero, following [15]. β is a non-negative weighting term which can be used to incorporate knowledge of the higher order moments of the distribution. Preliminary numerical analysis have shown that in our problem setting $\beta=0$ delivers the best estimates. At last, α controls the "size" of the Θ points distribution and should be $0 \leq \alpha \leq 1$. We choose $\alpha = \sqrt{3/p}$ in order to have the Θ_{ki} points in the center of Π_k facets. This choice allows for sharing some computations between adjacent Π_k sets, and thus to reduce the overall computational load.

3.2 Solution of Problem 1 on an LTV system

Consider a generic hyper-rectangular $\Pi_k \subseteq \Pi$. Π_k is a convex polytope having 2^p vertices $\pi^{(v)}$, i.e. admits the following vertex representation:

$$\Pi_k = \left\{ \pi \in \mathfrak{R}^p \mid \pi = \sum_{v=1}^{2^p} \lambda_{kv} \pi_k^{(v)}, \lambda_{kv} \geq 0, \sum_{v=1}^{2^p} \lambda_{kv} = 1 \right\}$$

Consider the LTV system obtained by linearization of the nonlinear system (1) around its trajectory under π_k^0 (Eq.(7)). Thanks to the superposition principle, any solution of the LTV system under a generic π in Π_k is a convex combination of the solutions under all the $\pi^{(v)}$. Furthermore, the λ_{kv} coefficients identifying the generic solution are equal to the ones identifying π in Π_k . All the output trajectories $y_{Lk}(t, \pi)$, with π ranging in Π_k , thus belong to the following set (tube) $S_{Lk}(t)$.

$$\pi \in \Pi_k \Rightarrow y_{Lk}(t, \pi) \in S_{Lk}(t),$$

$$S_{Lk}(t) = \left\{ y_{Lk}(t, \pi) \in \mathfrak{R}^m \mid y_{Lk}(t, \pi) = \sum_{v=1}^{2^p} \lambda_{kv} y_{Lk}(t, \pi_k^{(v)}), \right. \\ \left. \lambda_{kv} \geq 0, \sum_{v=1}^{2^p} \lambda_{kv} = 1 \right\}$$

As a consequence, the knowledge of the 2^p vertex trajectories $y_{Lk}(t, \pi_k^{(v)})$ allows to completely determine the region in which all the other trajectories are included. In this way, the system time response under any π in Π_k is completely characterized by a limited (and known a priori) number of trajectories, which can be obtained by numeric simulation. This allows obtaining a solution to Problem 1.

Consider the half-space representation of the reduced admissible solutions tube $S'_{R}(\cdot)$ (that can easily be obtained because $S'_{R}(\cdot)$ is hyper-rectangular by assumption).

$$S'_{R}(t) = \left\{ y \in \mathfrak{R}^m \mid S_R^A \cdot y \leq S_R^B(t) \right\}$$

Where ($I_{m \times m}$ stands for the m by m eye matrix):

$$S_R^A = \left(I_{m \times m} \mid -I_{m \times m} \right)^T, \quad S_R^B : [0, T] \rightarrow \mathfrak{R}^{2m \times 1}$$

Let us define the Boolean property P_k , such that it is defined only if the property P of Eq.(3) is globally definite (either 0 or 1) on Π_k :

$$P_k := \begin{cases} 1 & P(\pi) = 1 \quad \forall \pi \in \Pi_k \\ 0 & P(\pi) = 0 \quad \forall \pi \in \Pi_k \end{cases} \quad (12)$$

Given the convexity preserving nature of the LTV trajectories under constant inputs, the following hold, where $[\cdot]_i$ denotes the i -th row of a matrix:

$$\forall t \in [0, T], \forall v = 1, \dots, 2^p \\ S_R^A \cdot y_{Lk}(t, \pi_k^{(v)}) \leq S_R^B(t) \quad \Rightarrow \quad P_k = 1 \quad (13a)$$

$$\exists t \in [0, T], \exists i = 1, \dots, 2m: \forall v = 1, \dots, 2^p \\ [S_R^A]_i \cdot y_{Lk}(t, \pi_k^{(v)}) > [S_R^B(t)]_i \quad \Rightarrow \quad P_k = 0 \quad (13b)$$

Thus, by examining only the 2^p vertex trajectories $y_{Lk}(t; \pi^{(v)})$, one can determine if the robustness criterion P is satisfied globally on a given hyper-rectangular region Π_k . In case $P_k=0$, the robustness criterion is violated for all the uncertainties in Π_k , which is so identified as a region in which the system does not comply to the robustness criterion. At last, in case none of the conditions (13) is satisfied, this implies that the robustness criterion may hold only in a subset of Π_k . In this case, we can further bisect Π_k using the technique described in section 3.1, until either we find subsets in which P is globally definite, or we reach a minimum allowed measure of the Π_k sets, which is a maximum resolution at which the Π domain is analyzed.

Thus, Problem 1 is solved exactly for the LTV approximating systems defined on $\{\Pi_k\}_{Lin}$, and, due to the error tolerance ε , conservatively for the nonlinear system (1).

4 APPLICATION CASE

In order to ascertain the potentials of the proposed methodology, this section shows results obtained on a problem of practical engineering interest, relative to one of the test flights foreseen by the Unmanned Space Vehicle (USV) program, pursued by the Italian Aerospace Research Center (CIRA). In particular, it refers to the Dropped Transonic Flight Test (DTFT) [7], in which the FTB1 vehicle, developed as part of the USV program, is released from a stratospheric balloon at an altitude of 20 km, and performs an un-powered gliding flight reaching the transonic regime. The mission ends by deploying a parachute at a given Mach number, in order to safely splashdown in the Tyrrhenian Sea.

We apply the previously described method to perform the robustness analysis of the vehicle's longitudinal FCL. To this end, a purely longitudinal flight dynamics nonlinear model is considered, fed back by a gain scheduled PID longitudinal flight control loop itself commanded by a time-varying guidance law, and subject to uncertainties in the aerodynamic coefficients. Details of the model can be found in [16], and will be here omitted for brevity.

A detailed description of the FTB1 vehicle geometric and structural data can be found in [18]. According to the complete aerodynamic dataset, which is presented in [19], the lift, drag and pitching moment coefficients are given as the sum of a nominal and an uncertain aliquot. The former, obtained by interpolation of data given at discrete points of the flight envelope, foresees a nonlinear dependency on angle of attack α , Mach number M , altitude h , pitch rate q , and symmetric deflection of the elevons δ_e , which is the primary longitudinal control effector. Concerning the uncertain aliquot, only the three most influential uncertain parameters are herein taken into account. In particular, we consider bias uncertainties in drag and pitching moment coefficients along with the uncertainty in the effect of the elevons symmetric deflection on the pitching moment coefficient. The uncertainties influence on the relevant aerodynamic coefficient is modeled by means of non-dimensional scaling functions that depend on the Mach number. Following the current industrial practice, the scaling functions are taken equal to the maximum expected uncertainty range at each Mach number, also allowing normalizing to $[-1,1]$ the uncertain parameters ranges. The resulting aerodynamic coefficients functional dependencies are given in Eqs. (14), where the *nom* superscript denotes the nominal aerodynamic coefficient, and Fig. 1 shows the scaling functions profile.

$$C_L = C_L^{nom}(\alpha, M, h, q, \delta_e) \quad (14a)$$

$$C_D = C_D^{nom}(\alpha, M, h, \delta_e) + s_{D0}(M) \cdot \pi_{D0} \quad (14b)$$

$$C_m = C_m^{nom}(\alpha, M, h, q, \delta_e) + s_{m0}(M) \cdot \pi_{m0} + \delta_e \cdot s_{m\delta}(M) \cdot \pi_{m\delta} \quad (14c)$$

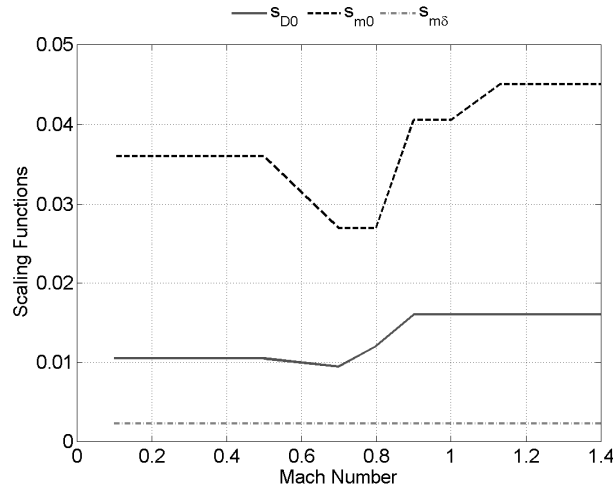


Fig. 1 Scaling functions for aerodynamic uncertainties modeling.

After the first few seconds of the initial drop phase, in which the elevons do not have sufficient command authority due to the very low dynamic pressure, the vehicle dynamics are augmented by a PID FCL, arranged in a cascade structure with feedback on pitch rate and angle of attack. The FCL gains k are scheduled with respect to the dynamic pressure throughout the flight profile. The time-varying guidance law in angle of attack α_{ref} , shown in Fig. 2, commands the augmented dynamics. The overall feedback action can be expressed as follows.

$$\delta_e = k_3 \left[k_1 (\alpha_{ref} - \alpha) + \dot{\xi} - q \right] ; \dot{\xi} = k_1 k_2 (\alpha_{ref} - \alpha) \quad (15)$$

$$k_1 = k_{10} + k_{1s} q_\infty ; k_2 = k_{20} + k_{2s} q_\infty ; k_3 = k_{30} + k_{3s} / q_\infty \quad (16)$$

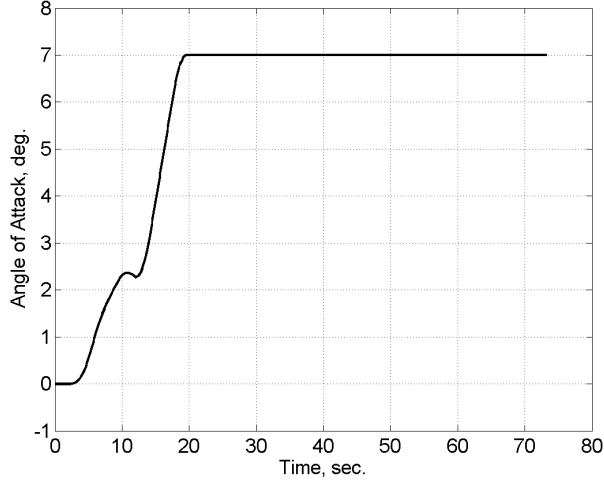


Fig. 2 Angle of attack reference guidance law

Introducing the aerodynamic coefficients model of Eq. (14) in the open-loop longitudinal dynamics, and substituting Eq. (15) for δ_e , we can recast the augmented vehicle dynamics in the form of Eq.(1), in which $x = (V \ \alpha \ \theta \ q \ h \ r \ \xi)^T$, $y = (\alpha \ M \ \delta_e)^T$, $\pi = (\pi_{D0} \ \pi_{m0} \ \pi_{m\delta})^T$, where V stands for the air relative velocity, θ for the pitch angle, and r for the flown range.

The presented method has been applied to analyze this nonlinear system up to $T = 73$ sec., which is representative of the overall mission duration. The initial value of the system state is equal to $x|_{t=0} := (0.01 \text{ m/sec.}; 0 \text{ deg.}; -90 \text{ deg.}; 0 \text{ deg/sec.}; 20000 \text{ m}; 0 \text{ m}; 0 \text{ deg./sec.})^T$. Three robustness criteria are enforced, based on mission requirements and FCL performance metrics. The FCL is required to track the reference angle of attack time-history with at most a 2 deg. error, as well as to avoid issuing commands to the actuation system beyond its maximum capabilities. The latter requirement is enforced requiring δ_e to remain within $[-25, 25]$ deg. At last, the Mach number is limited from above and below in the transonic region due to the mission objectives. These three robustness criteria define a time-varying hyper-rectangular admissible solutions tube in a very straightforward manner, whose one-dimensional projections in the three output variables are shown in Fig. 3.

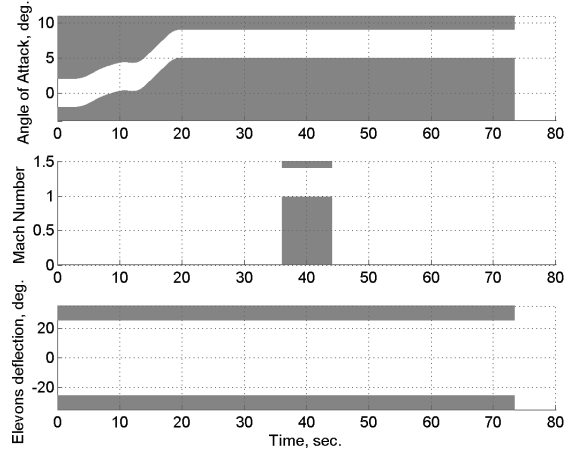


Fig. 3 One dimensional projections of S_R (in white)

A candidate FCL tuning, determined by means of conventional LTI-based synthesis techniques, is now analyzed using the proposed approach. Its gains vary according to Eq. (16) with $k_{I0} = 1 \text{ sec}^{-1}$; $k_{I5} = 0$; $k_{20} = -3,77 \cdot 10^{-1} \text{ sec}^{-1}$; $k_{2s} = 4,55 \cdot 10^{-4} \text{ m} \cdot \text{sec} \cdot \text{kg}^{-1}$; $k_{30} = 3,01 \cdot 10^{-2} \text{ sec}$; $k_{3s} = -4,03 \cdot 10^3 \text{ kg} \cdot \text{sec}^{-1} \cdot \text{m}^{-1}$. The linearization phase results are collected in Fig. 4, showing $\{\Pi_k\}_{Lin}$, the partition into which the uncertainties domain Π has been divided to obtain a meaningful approximation. In each Π_k belonging to $\{\Pi_k\}_{Lin}$ the nonlinear dynamics are numerically linearized around their trajectory under π_k^0 . In this specific application, the nonlinear system is successfully approximated in all Π within the allowed resolution. Fig. 5 collects the robustness analysis results, in which three different areas can be identified. The gray one including all the subsets Π_k in which the criterion is cleared, i.e. $P_k = 1$. Given the previous discussions, this region conservatively approximates Π_{Adm} . The white one is instead made of all the subsets with the minimum allowed size, in which no definite clearance information can be obtained without further partitioning. At last, the black region is made of all the subsets Π_k in which the criterion is not cleared, pointing out a substantial subset of Π in which the system robustness does not satisfy the criterion.

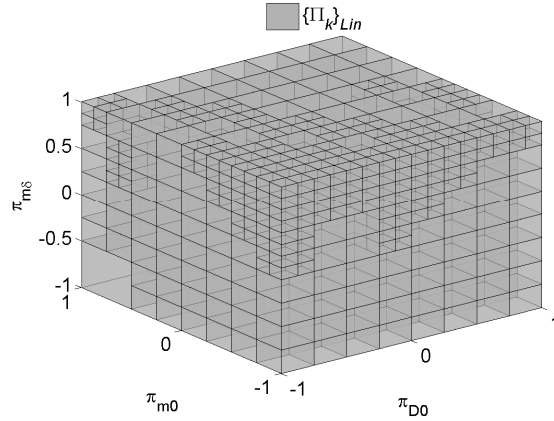


Fig. 4 Uncertainties domain partition for system linearization – $\{\Pi_k\}_{Lin}$

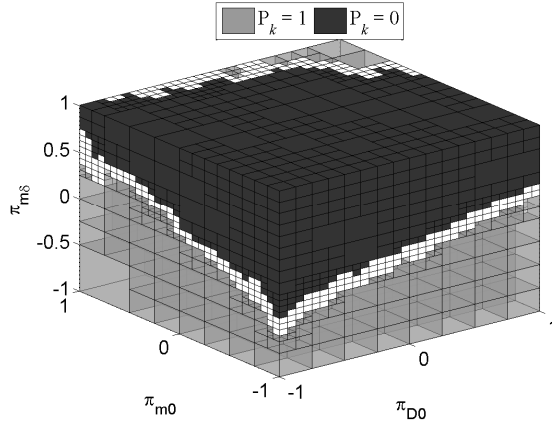


Fig. 5 Robustness criterion mapping in Π

As previously emphasized, one of the main advantages of the proposed approach is the capability to support the physical understanding of all the causes for unsatisfactory FCL robustness within Π . One outcome of the analysis that is instrumental in achieving this objective is the capability to estimate conservatively the dispersion of the nonlinear trajectories. More precisely, all the nonlinear trajectories resulting from a given continuous region within the uncertainties domain may be enclosed by a tube computed using information only in a finite number of suitably selected points. Indeed, given a generic sub-partition $\{\Pi_k\}$, the nonlinear system solutions tube arising from all the uncertainties combinations in $\{\Pi_k\}$ is included in the Minkowski sum between the tolerance ball B_ε and the union of all the tubes of the relevant blocks (see section 3). The latter, being a union of polytopes, is itself included in the convex hull of all the vertex trajectories of the tubes. In addition, since convexity is preserved under projection, these convex hulls and the Minkowski addition may be computed directly in any low dimension regardless of the output space dimension, thus requiring limited computational resources. This allows to efficiently build graphical representations of the nonlinear trajectories dispersion that considerably aid results interpretation. Indeed, Fig. 6 and Fig. 7 show the one-dimensional projections in α , M , and δ_e of the estimate of the nonlinear solutions tube for π belonging to the Π_k subsets for whom $P_k = 0$ (that is, the black region in Fig. 5), at a series of simulation time epochs, along with S_R .

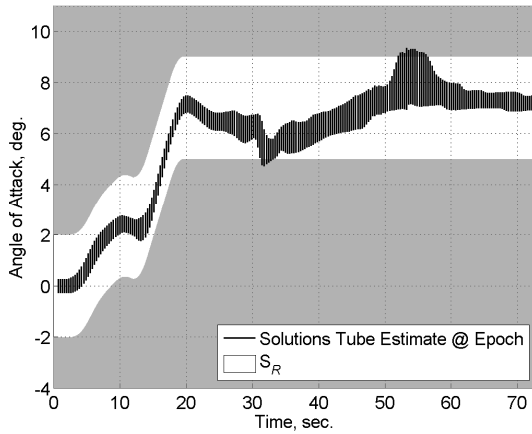


Fig. 6 Projection in α of the solutions tube estimate for $P_k = 0$ vs. S_R .

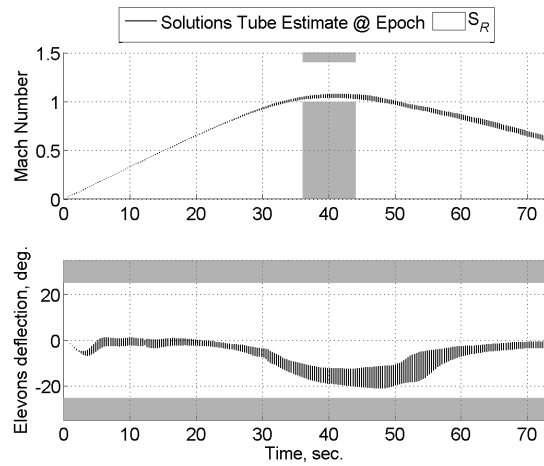


Fig. 7 Projections in M and δ_e of the solutions tube estimate for $P_k = 0$ vs. S_R .

Whilst both the Mach number and the elevons deflection robustness criteria are matched, the angle of attack tracking performance is unsatisfactory. More precisely, two distinct violations are observed: one due to an excessively low angle of attack when entering the transonic regime, the other one due to an excessively high angle of attack when returning to subsonic conditions. These oscillations are both caused by a sharp decrease of the elevons efficiency in the transonic phase. However, because of the considerable uncertainty on the entity of this phenomenon, no dedicated feed-forward actions were implemented. The influence of the uncertain parameters on the two oscillations are different, because of the asymmetry of the α profile. In order to assess this difference, a further analysis has been performed separating the two oscillations. This may be achieved modifying the admissible solutions tube definition, once enforcing only the lower tracking bound on α , and once the higher. We emphasize that, since the results of the approximation phase do not depend on the admissible solutions tube, these additional analyses require performing only the property clearance phase. This does not involve any nonlinear simulations or numeric linearization, thus has an execution time considerably smaller than the linearization one. The new property clearance results are shown in Fig. 8 and Fig. 9 for the lower and higher α tracking bounds, respectively.

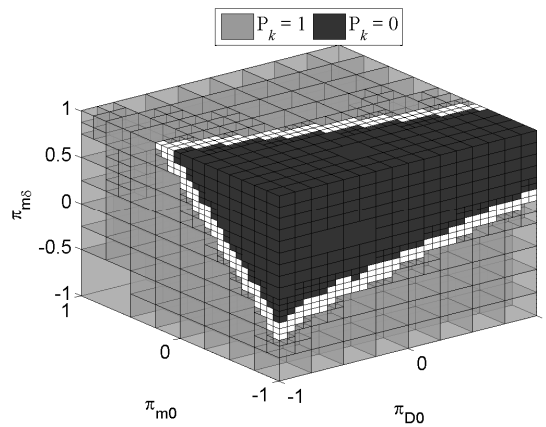


Fig. 8 Robustness criterion mapping in Π ; lower α tracking bound only.

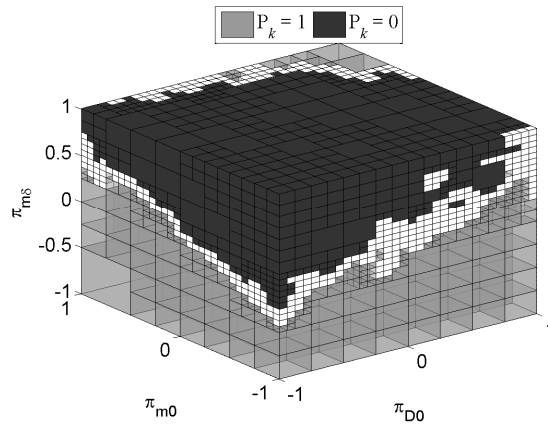


Fig. 9 Robustness criterion mapping in Π ; upper α tracking bound only.

Results indicate that the first oscillation may extend below the α tracking requirement when a decrease in the pitching moment is coupled with an increase in the elevons effect on the pitching moment. These two factors are clearly predominant with respect to the drag bias uncertainty within the expected uncertainties ranges. On the other hand, the drag bias uncertainty has an effect comparable to the pitching moment bias one in affecting the post-transonic oscillation, whose compliance to the α tracking requirement is considerably influenced by the elevons effect on the pitching moment. It is evident how the physical phenomenology underlying the α tracking requirement violation in dispersed conditions is different for the pre- and post-transonic phases, implying that the eventual FCL design refinement should be conducted with regard to multiple test cases. This typical situation highlights the benefits of the proposed approach when compared to the optimization-based worst-case search. This, in spite of the capability of identifying the uncertainties combination yielding the worst value of the robustness criterion, may indeed fail to support the subsequent FCL refinement when multiple violations of the criterion are present, arising from different causes calling for diverse FCL refinement strategies.

Based on the regions identified in the previous analyses, the FCL design has been upgraded by means of conventional techniques, yielding a modified gain tuning. In particular, the proportional gain on the angle of attack k_I has been increased in the early phases of flight ($k_{I0} = 2,00 \text{ sec}^{-1}$; $k_{Is} = -6,00 \cdot 10^{-5}$), to recover the first oscillation. The post-transonic oscillation issues were instead relieved by decreasing the gain on the pitch rate k_q in the high-dynamic pressure flight conditions ($k_{30} = -2,00 \cdot 10^{-1} \text{ sec}^{-1}$; $k_{3s} = -6,50 \cdot 10^3 \text{ kg} \cdot \text{sec}^{-1} \cdot \text{m}^{-1}$). An additional analysis, whose results are shown in Fig. 10 to Fig. 12, has been performed, showing that the new FCL tuning exhibits satisfactory robustness to the uncertainties taken into account.

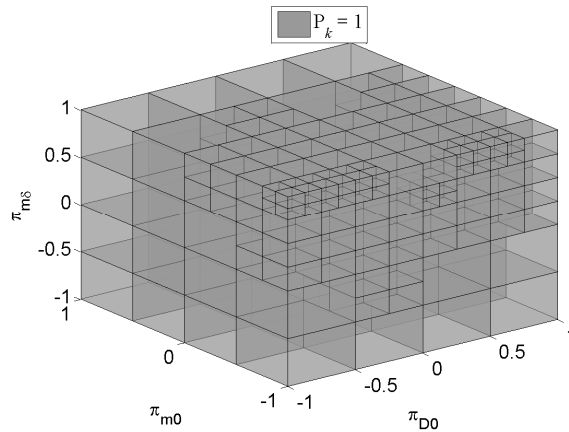


Fig. 10 Robustness criterion mapping in Π .

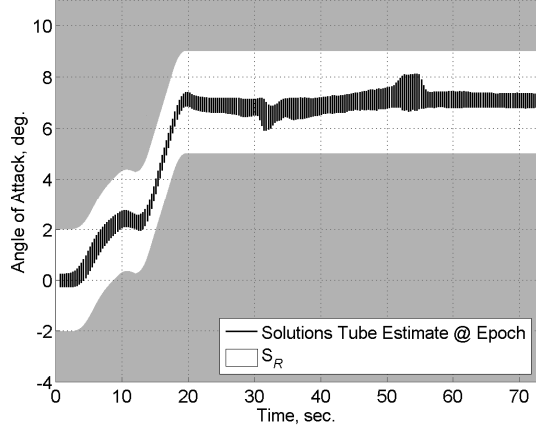


Fig. 11 Projection in α of the solutions tube estimate for π in Π vs. S_R .

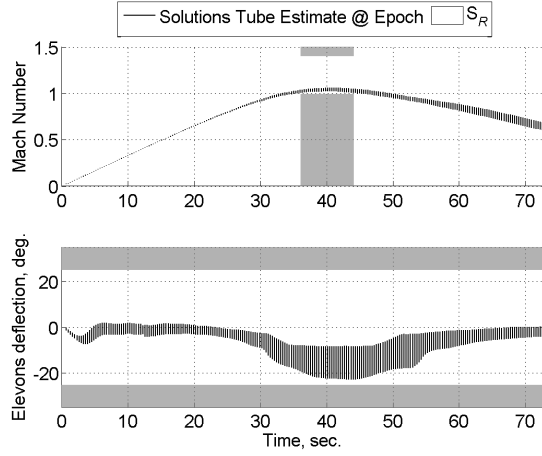


Fig. 12 Projections in M and δ_e of the solutions tube estimate for π in Π vs. S_R .

The application presented in this section highlights the potentials of the proposed approach in supporting the FCL refinement process. Concerning the execution time, these results were obtained in ~ 12 minutes using a standard desktop PC equipped with a Pentium IV 2.4 GHz processor and 2GB RAM. To give a term of comparison, numerically evaluating the robustness criterion (3) by a brute-force approach on a uniformly spaced grid at the same resolution takes more than 4 hours. However, it is emphasized that information delivered by the two methods is different since brute-force methods give results valid only in the grid nodes, thus calling for higher resolutions. On the contrary, the proposed method's results apply continuously in the uncertainties domain, allowing to take advantage of relatively low resolutions.

At last, we provide an insight of the performance of the SUT in guaranteeing that the nonlinear trajectories approximation error is below the desired threshold in this application case. In particular, we draw a series of $N = 7000$ random samples of π , uniformly distributed over Π . We then numerically evaluate the $d(\cdot)$ function on these samples, using the LTV approximations defined on the previously computed $\{\Pi_k\}_{Lin}$. The so obtained $d(\cdot)$ values are shown in Fig. 13, and compared to the error tolerance ϵ .

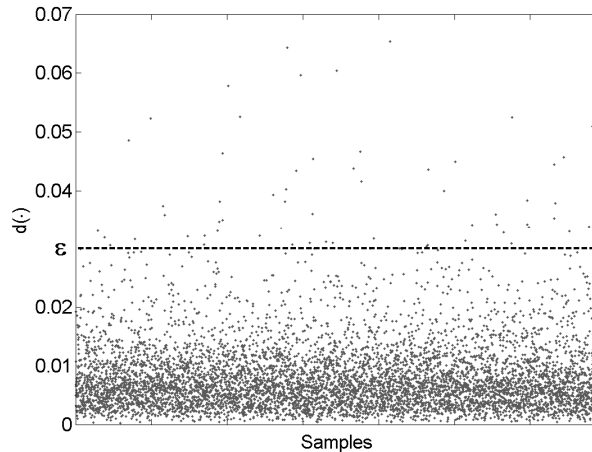


Fig. 13: Random evaluation of $d(\cdot)$ function on $\{\Pi_k\}_{Lin}$

It is seen that $d(\cdot)$ is effectively smaller than ϵ in most of Π . The probability of $d(\cdot)$ being higher than the tolerance may be estimated as the ratio between the number of samples in which $d > \epsilon$ and the total number of samples, yielding $\Pr\{d > \epsilon\} \approx 0.009$. These results are consistent with the 6% value that has been specified in section 3.1.1 for the risk of $d(\cdot)$ being higher than the error tolerance, and thus confirm that the SUT is adequate for evaluating the approximation error in estimating the nonlinear trajectories with those of its linearizations.

5 CONCLUSION

A novel approach to flight control laws robustness analysis for vehicles following time-varying reference trajectories under parametric uncertainties has been proposed. Main advantages with respect to conventional clearance techniques include, but are not limited to, coherence in the robustness criterion formulation, with a resulting higher confidence in the analysis results, the capability of dealing with advanced FCL, to which conventional techniques poorly apply, and a bounded, and reducible, amount of conservatism.

A nonlinear robustness criterion has been developed and formulated as a Practical Stability analysis problem. A novel approach is pursued, which approximates the original nonlinear system by a certain number of its time-varying linearizations, numerically obtained by means of a recursive partitioning technique of the uncertainty domain. In particular, suitability of the LTV approximating systems is evaluated in a probabilistic fashion making use of the Unscented Transformation technique. Then, the practical stability analysis is performed by means of a deterministic approach exploiting the convexity-preserving nature of LTV systems. As a result, we obtain a hybrid probabilistic – deterministic approach, capable of solving the defined robustness analysis problem with no heuristic assumptions.

The method potentials in increasing the efficiency of the FCL robustness analyses is addressed by application to the longitudinal flight control law of CIRA experimental vehicle USV. Results are presented in terms of determining the subsets of the expected uncertainties' domain within which adequate performance of the augmented vehicle is verified. Comparison with conventional clearance methods suggests the viability of the proposed method, also in terms of sustainable computational load.

REFERENCES

- [1] Khalil, H. K., Nonlinear Systems. 3rd ed., Prentice Hall, Upper Saddle River, NJ, 2002, Chap. 9.
- [2] Lee, H. C., Choi, J. W., "Linear Time-Varying Eigenstructure Assignment with Flight Control Application." IEEE Transactions on Aerospace and Electronic Systems, Vol. 40, No. 1, pp. 145- 157, 2004.
- [3] Gamble, J.D., The Application of Aerodynamic Uncertainties in the Design of the Entry Trajectory and Flight Control System of the Space Shuttle Orbiter. Shuttle Performance : Lessons Learned, NASA CP 2283 Part I, Hampton, VA., 1983.
- [4] Dorato, P., An Overview of Finite-Time Stability, in: L. Menini, L. Zaccarian, C. T. Abdallah (eds.), Current Trends in Nonlinear Systems and Control: In Honor of Petar Kokotovic and Turi Nicosia, Birkhauser Boston, 2006, pp 185-195.

- [5] Tancredi, U., Grassi, M., Corrado, F., Filippone, E., Palumbo, R., Russo, M., A Novel Method for Flight Control Laws Robustness Analysis over Unsteady Trajectories, Proc. of the 17th IFAC Symposium on Automatic Control in Aerospace, June 2007, Toulouse, France
- [6] Julier, S., Uhlmann, J., Durrant-Whyte, H.F., A new method for the nonlinear transformation of means and covariances in filters and estimators, IEEE Transactions on Automatic Control, vol. 45, no. 3, pp. 477-482, 2000.
- [7] Pastena, M., Di Donato, M., Palma, et al. "PRORA USV1: The First Italian Experimental Vehicle to the Aerospace Plane," AIAA/CIRA 13th International Space Planes and Hypersonics Systems and Technologies Conference, AIAA-2005-3348, Capua, Italy, 2005.
- [8] Gruyitch, L., Richard, J-P., Borne P., Gentina, J.C., Stability Domains, Chapman & Hall/CRC, 2000, Chaps. 1,2, 6.
- [9] Ryali, V., Moudgalya, K.M., "Practical stability analysis of uncertain nonlinear systems", National Conference on Control and Dynamic Systems, IIT Bombay, 27-29 January 2005.
- [10] Asarin, E., Dang, T., Girard, A., Hybridization methods for the analysis of nonlinear systems, Acta Informatica, Vol.43, n.7, 451-476, 2007.
- [11] Desoer, C. A., Vidyasagar, M., Feedback systems: input-output properties, Academic Press, Inc., New York, 1975, Chap. 4.
- [12] Kihias, D., Marquez, H. J., Computing the distance between a nonlinear model and its linear approximation: an L2 approach, Computers and Chemical Engineering, Vol. 28, No. 12, pp. 2659-2666, 2004.
- [13] Rewienski, M., White, J., A Trajectory Piecewise – Linear Approach to Model Order Reduction and Fast Simulation of Nonlinear Circuits and Micromachined Devices, Proceedings of the 2001 IEEE/ACM international conference on Computer-aided design, San Jose, California, 252 – 257, 2001.
- [14] Julier, S. J., and Uhlmann, J. K., The scaled unscented transformation, Proceedings of the American Control Conference, pp. 4555-4559, 2002.
- [15] Van der Merwe, R., De Freitas, N., Doucet, A., and Wan, E. A., The Unscented Particle Filter, in: Leen, T. K., Dietterich, T. G., Tresp, V. (Eds.), Advances in Neural Information Processing Systems (NIPS13), MIT Press, 2000.
- [16] Tancredi, U., Grassi, M., Corrado, F., Filippone, E., Russo, M., A Novel Approach to Clearance of Flight Control Laws over Time Varying Trajectories, Automatic Control in Aerospace online Journal, ISSN 1974-5168, Vol.1, n.1, 2008.
- [17] Corrado, F., Filippone, E., Russo, M., Verde, L., Tancredi, U., Moccia A., Grassi, M., "Flight Dynamic Characterisation of the USV-Flying Test Bed Vehicle ", AIAA/CIRA 13th International Space Planes and Hypersonics Systems and Technologies Conference, AIAA-2005-3276, Capua, Italy, May 16-20, 2005
- [18] Tancredi, U., Grassi, M., Moccia, A., Verde L., and Corrado, F., Allowable Aerodynamics Uncertainties Synthesis Aimed at Dynamics Properties Assessment for an Unmanned Space Vehicle, AIAA Paper 2004-6582, 2004.
- [19] Rufolo, G., Roncioni, P., Marini, M., Votta, R., and Palazzo, S., Experimental and Numerical Aerodynamic Data Integration and Aerodatabase Development for the PRORA-USV-FTB_1 Reusable Vehicle, AIAA Paper 2006-8031, Canberra, Australia, 2006.